Supplementary Information

Mutant p63 causes defective expansion of ectodermal progenitor cells and impaired FGF signaling in AEC syndrome.

Giustina Ferone, Helen A. Thomason, Dario Antonini, Laura De Rosa, Bing Hu, Marica Gemei, Huiqing Zhou, Raffaele Ambrosio, David P. Rice, Dario Acampora, Hans van Bokhoven, Luigi Del Vecchio, Maranke I. Koster, Gianluca Tadini, Bradley Spencer-Dene, Michael Dixon, Jill Dixon, and Caterina Missero.

Table of content

Supplementary Materials and Methods 3

References 7

Figure S1. p63 expression in *p63*$^{+/L514F}$ mice 9

Figure S2. Craniofacial abnormalities in *p63*$^{+/L514F}$ mice 10

Figure S3. Skin defects and ectodermal dysplasia in *p63*$^{+/L514F}$ mice 11

Figure S4. Stratification and skin barrier formation in *p63*$^{+/L514F}$ embryos 12

Figure S5. Apoptosis in *p63*$^{+/L514F}$ epidermis 13

Figure S6. Expression of cell cycle regulators in *p63*$^{+/L514F}$ E14.5 skin or keratinocytes 14

Figure S7. Identification of p63 binding regions in the *Fgfr2* gene locus 15

Figure S8. Identification of p63 binding regions in the *Fgfr3* gene locus 16

Figure S9. ERK phosphorylation in *p63*$^{+/L514F}$ keratinocytes 18

Figure S10. Analysis of S-phase of the cell cycle in *p63*$^{+/L514F}$ keratinocytes 19

Table S1. Microarray analysis of p63 target genes 20

Table S2. Microarray analysis of FGF signaling components encoding genes 21

Table S3. Mutations in AEC patients used in this study 22

Table S4. List of oligonucleotide primers 23

Supplementary Materials and Methods

Generation of the p63$^{+/L514F}$ ES cells, ES and mouse screening

L514F mutation was inserted into the *p63* locus in E14TG2a ES cells by recombineering (Liu et al, 2003). A portion of the *p63* gene from exon 12 to the 3'UTR was subcloned into a pBluescript vector (pBS) DNA from mouse BAC clone bMQ-241L2 via gap repair, essentially as previously described (Liu et al, 2003). Miniarms were cloned into the *Not*I and *Spe*I sites of pBS using *Not*I-p63ex12For and *Hin*dIII-p63ex12Rev, and *Hin*dIII-p63-3'UTRFor and *Spe*I-p63-3'UTRRev oligonucleotide primers. The vector was subsequently linearized with *Hin*dIII and electroporated into the recombinogenic bacterial strain EL350 containing the bMQ-241L2 BAC clone to obtain the repaired vector. The positive selection marker PGK-Neo and exon 13 containing the diagnostic *Eco*RI site and the TTA to TTT mutation (L514F) was inserted in one recombineering step. Mutant exon 13 was amplified by PCR from a pCMV-FLAGmouse p63 L514F with *Not*I-ex13For and *Eco*RI-ex13Rev primers. Intron 13 was PCR-amplified from the repaired vector with *Bam*HI-intron13For and *Sal*I-intron13Rev primers. The PCR amplified regions were inserted by cloning in the pL251 vector containing the PGK-Neo cassette. The resulting minitargeting vector was digested with *Not*I -*Sal*I and electroporated in EL350 *E. Coli* bacterial strain together with the repaired vector containing the *p63* sequence. The final vector containing a PGK-neo cassette flanked by loxP sites and the L514F point mutation in exon 13 was electroporated into mouse E14Tg2A (129/Ola) ES cells. Twenty-four hours after electroporation ES cells were selected with 100 μg/ml G418 (Invitrogen) for 7 days. Neo-resistant ES clones were screened at 3' and 5' for the correct insertion in the *p63* endogenous locus by PCR analysis using an oligonucleotide annealing in the neomycin cassette and an one annealing in the genomic DNA (5' insertion: EsScreen5'For and EsScreen5'Rev primers; 3' insertion: EsScreen3'For and EsScreen3'Rev primers). The homologous recombination event was confirmed by Southern blotting.

Genomic DNA was digested with *Eco*RI and analyzed with a probe located

upstream of the recombinant targeted site. The wild-type allele resulted in a band of 5392 bp. The recombinant ES clone contained the wild-type band as well as a recombinant band of 3216 bp, due to insertion of a diagnostic *Eco*RI site at the 5' end of PGK-Neo cassette and thus consistent with the homologous recombination event. The presence of the mutation in the endogenous locus was confirmed by sequencing of ES genomic DNA. An ES positive clone was injected into C57BL/6 blastocysts, and six chimeras from a first injection and ten chimeras from a second injection were obtained. The chimeras were all tested for germline transmission by breeding with C57BL/6 females, and were subsequently bred with female mice from C57BL/6, or BALB/c, DBA/1, CBA, 129/Sv and C3H strains in an attempt to rescue the lethal phenotype. Offspring was genotyped for germline transmission of the $p63^{L514F}$ wild-type and mutant allele by PCR using tail genomic DNA and specific primers (Screen-ex13L514F-For and Screen-ex13L514-wild-type-Rev or Screen-ex13L514F-Mut-Rev). $p63^{+/-}$ mice were obtained from Jackson Laboratory (Mills et al, 1999).

Skin Barrier Assay

To perform X-gal staining, unfixed embryos were washed in PBS and then incubated overnight at 37 °C in 5-bromo-4-chloro-3-indlyl-b-D-galactopyranoside (X-gal) reaction mix (100 mM NaPO4, 1.3 mM MgCl2, 3 mM K3Fe[CN]6, 3 mM K4Fe[CN]6, and 1 mg/ml X-gal [pH 4.5]). Since skin cells have endogenous ß-galactosidase activity, increased staining indicates epidermal permeability to X-gal, a sign of compromised barrier function.

Skeletal preparation

To analyze the whole skeleton newborn mice were dissected to remove skin, muscle, and fat and kept in acetone to remove further fat for 3 days. They then were stained with 0.09% alizarin red S and 0.05% Alcian blue in a solution containing ethanol, glacial acetic acid, and water (67:5:28) for 48 h at 37°C. After staining, mice were transferred to 1% potassium hydroxide until the skeleton was

clearly visible. Mice were preserved in 100% glycerol with gradual increase in concentration.

Antibodies

The following primary antibodies were used for immunofluorescence and immunoblotting: Rabbit polyclonal for Krt14, Krt1, Krt10, involucrin and loricrin (Covance), Krt17 (kindly provided by Pierre Coulombe), FGFR2 (C-17, Santa Cruz Biotechnology), phospho-FRS2α Tyr196 (Cell Signaling Technology), FGFR3 (D2G7E, Cell Signaling Technology), Sox9 (H-90, Santa Cruz Biotechnology), phospho-Histone H3 (Ser10) (06-570, Millipore), $p57^{Kip2}$ (H-19, Santa Cruz Biotechnology) caspase 3 active (R&D systems); mouse antibodies to BrdU G3G4 (originally provided by Dr. Steve J. Kaufman, Illinois and maintained by the Developmental Studies Hybridoma Library, University of Iowa), p63 (4A4, Santa Cruz Biotechnology), α-tubulin (Sigma); rat antibodies to E-cadherin (Invitrogen) and to Krt8 (TROMA 1 developed by Philippe Brulet and Rolf Kemler, and maintained by the Developmental Studies Hybridoma Bank); guinea pig antibody to Krt15 (kindly provided by Lutz Langbein); goat antibody to Sox2 (AF2018, R&D Systems).

For FACS analysis, freshly isolated newborn keratinocytes were stained for 20 min with phycoerythrin (PE)-conjugated anti-CD49f and FITC-conjugated anti-CD71 (transferrin receptor) primary antibodies (BD Biosciences) or FITC-conjugated anti-annexin V primary antibody (BD Biosciences).

The following primary antibodies were used for ChIP analysis: rabbit antibody for p63 (H137, Santa Cruz Biotechnology), rabbit anti-mouse IgG (Santa Cruz Biotechnology), rabbit polyclonal to Histone H3 monomethyl lys4 (Abcam-ab8895), rabbit polyclonal to Histone H3 trimethyl lys4 (Upstate 07-473), rabbit polyclonal to Histone H3 dimethyl lys4 (Upstate 07-030).

Secondary antibodies used for immunofluorescence staining: Alexa Fluor ® 488 goat anti-mouse (Invitrogen), Alexa Fluor ® 594 goat anti-rabbit (Invitrogen), Alexa Fluor ® 594 goat anti-rat (Invitrogen), Goat anti-Guinea Pig IgG secondary antibodies conjugated to FITC (Pierce).

Secondary antibody used for immunoblotting: donkey anti-rabbit and sheep anti-mouse IgG conjugated to horseradish peroxidase (HRP) (1:2000; Amersham Biosciences); donkey anti-goat HRP and goat anti-rat HRP (1:1000; Santa Cruz Biotechnology).

Human subjects

Heterozygous mutations have been described by Rinne and coworkers (Rinne et al, 2009) and are listed in Table 2. Mutation C519R has been identified by CEINGE Sequencing Core for mutation analyses from a patient identified by G.T. The Institutional Review Boards for Human Subject Research approved the research study. Written, informed consent was obtained from the parents of all children younger than 18 years and directly from all individuals 18 years of age or older.

Microarray analysis

We measured global changes in gene expression by microarray analysis on freshly isolated E14.5 skin from wild-type and $p63^{+/L514F}$ embryos, E18.5 epidermis, and primary keratinocytes cultured under growing conditions for one week. Three (E18.5 epidermis) or two (E14.5 skin, keratinocytes) independent mutant RNA and corresponding wild-type samples were analyzed by Affymetrix mouse 430A array at Coriell Institute (Camden, NJ, USA). The data generated underwent quality control and analysis using as previously described (Della Gatta et al, 2008). The entire dataset of microarray data will be published elsewhere (Ferone et al., manuscript in preparation).

Whole mount in situ hybridization.

Paraformaldehyde-fixed embryos at E14.5 were processed as described previously (Laurikkala et al, 2001). The digoxigenin-labelled probes were detected with NBT/BCIP Solution (Roche). The EDAR and Wnt10B probes were a kind gift of Andrzej A. Dlugosz (University of Michigan, USA) and Lef1 probe was a kind gift of Michéle Studer (University of Nice, France) and have been

described (Laurikkala et al, 2001; Zhang et al, 2009).

Statistics.

Statistical significance of the gene expression studies was assessed by unpaired 2-tailed Student's *t* test. p-values are indicated in Figure Legends. All quantitative results are presented as mean ± SD or SEM as indicated in the Figure Legends, as calculated by Excel software.

REFERENCES

Antonini D, Russo MT, De Rosa L, Gorrese M, Del Vecchio L, Missero C (2010) Transcriptional repression of miR-34 family contributes to p63-mediated cell cycle progression in epidermal cells. *The Journal of investigative dermatology* **130:** 1249-1257

Birney E, Stamatoyannopoulos JA, et al (2007) Identification and analysis of functional elements in 1% of the human genome by the ENCODE pilot project. *Nature* **447:** 799-816

Della Gatta G, Bansal M, Ambesi-Impiombato A, Antonini D, Missero C, di Bernardo D (2008) Direct targets of the TRP63 transcription factor revealed by a combination of gene expression profiling and reverse engineering. *Genome research* **18:** 939-948

Huang YP, Kim Y, Li Z, Fomenkov T, Fomenkov A, Ratovitski EA (2005) AEC-associated p63 mutations lead to alternative splicing/protein stabilization of p63 and modulation of Notch signaling. *Cell Cycle* **4:** 1440-1447

Kouwenhoven EN, van Heeringen SJ, Tena JJ, Oti M, Dutilh BE, Alonso ME, de la Calle-Mustienes E, Smeenk L, Rinne T, Parsaulian L, Bolat E, Jurgelenaite R, Huynen MA, Hoischen A, Veltman JA, Brunner HG, Roscioli T, Oates E, Wilson M, Manzanares M, Gomez-Skarmeta JL, Stunnenberg HG, Lohrum M, van Bokhoven H, Zhou H (2010) Genome-wide profiling of p63 DNA-binding sites identifies an element that regulates gene expression during limb development in the 7q21 SHFM1 locus. *PLoS Genet* **6:** e1001065

Laurikkala J, Mikkola M, Mustonen T, Aberg T, Koppinen P, Pispa J, Nieminen P, Galceran J, Grosschedl R, Thesleff I (2001) TNF signaling via the ligand-receptor pair ectodysplasin and edar controls the function of epithelial signaling centers

and is regulated by Wnt and activin during tooth organogenesis. *Developmental biology* **229:** 443-455

Liu P, Jenkins NA, Copeland NG (2003) A highly efficient recombineering-based method for generating conditional knockout mutations. *Genome research* **13:** 476-484

Mills AA, Zheng B, Wang XJ, Vogel H, Roop DR, Bradley A (1999) p63 is a p53 homologue required for limb and epidermal morphogenesis. *Nature* **398:** 708-713

Paus R, Muller-Rover S, Van Der Veen C, Maurer M, Eichmuller S, Ling G, Hofmann U, Foitzik K, Mecklenburg L, Handjiski B (1999) A comprehensive guide for the recognition and classification of distinct stages of hair follicle morphogenesis. *The Journal of investigative dermatology* **113:** 523-532

Rinne T, Bolat E, Meijer R, Scheffer H, van Bokhoven H (2009) Spectrum of p63 mutations in a selected patient cohort affected with ankyloblepharon-ectodermal defects-cleft lip/palate syndrome (AEC). *American journal of medical genetics* **149A:** 1948-1951

Sathyamurthy A, Freund SM, Johnson CM, Allen MD, Bycroft M (2011) Structural basis of p63alpha SAM domain mutants involved in AEC syndrome. *FEBS J* **278:** 2680-2688

Zhang Y, Tomann P, Andl T, Gallant NM, Huelsken J, Jerchow B, Birchmeier W, Paus R, Piccolo S, Mikkola ML, Morrisey EE, Overbeek PA, Scheidereit C, Millar SE, Schmidt-Ullrich R (2009) Reciprocal requirements for EDA/EDAR/NF-kappaB and Wnt/beta-catenin signaling pathways in hair follicle induction. *Dev Cell* **17:** 49-61

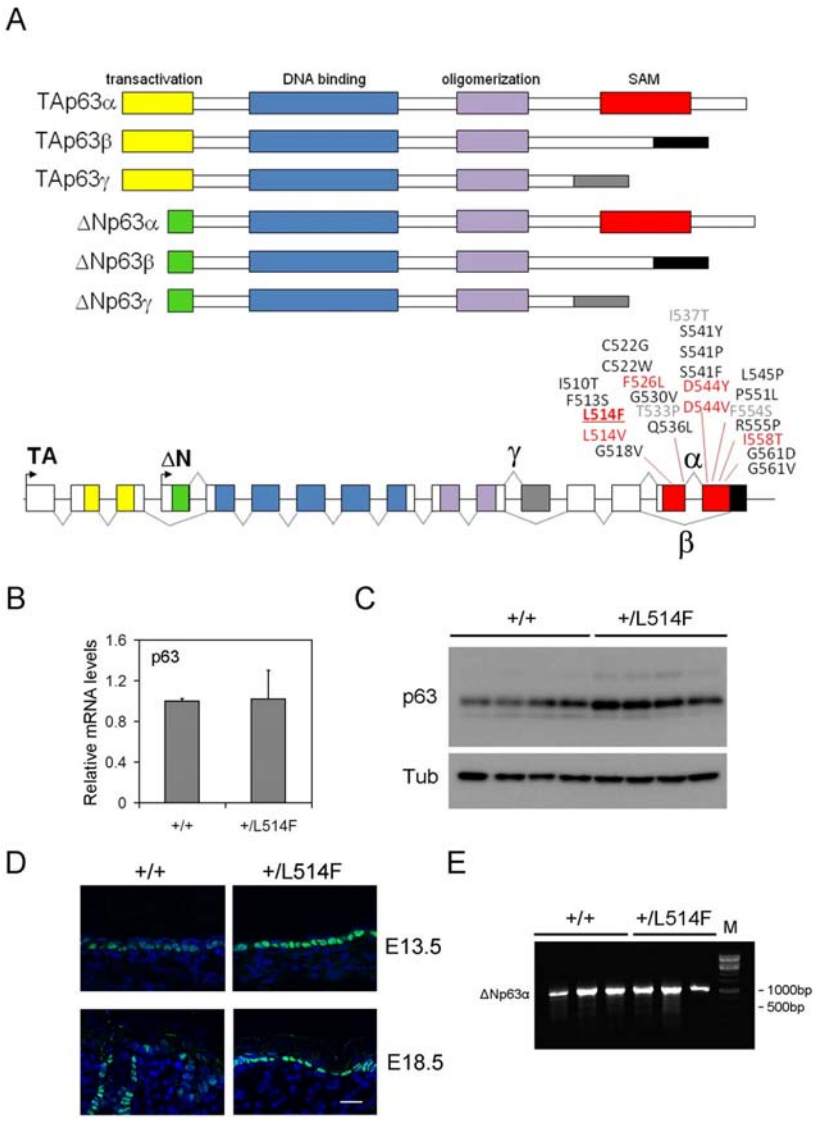

Figure S1. p63 expression in *p63*$^{+/L514F}$ mice. (**A**) Schematic representation of p63 protein isoforms (upper panel) and *p63* gene with AEC mutations in portion encoding the SAM domain. Residues that are absolutely conserved are shown in red. Conserved and partially conserved hydrophobic residues are shown in black and grey, respectively (Sathyamurthy et al, 2011). (**B**) Real time RT-PCR from E14.5 skin mRNA reveals similar expression of *p63* in *p63*$^{+/L514F}$ compared to wild-type (+/+) controls. Values are expressed as ß-actin normalized mRNA levels and are the mean of 8 independent skin samples. Error bars represent standard deviation (SD). (**C**) p63 protein expression in newborn epidermis. α–Tubulin was used as loading control. (**D**) Confocal imaging of a p63 immunofluorescence performed at limiting antibody dilution (1:1000) of E13.5 and E18.5 skin. Scale bar: 20 µm. (**E**) RT-PCR analysis of the 3' region of p63 mRNA from newborn epidermis was performed to detect a previously described aberrant splicing isoform

(Huang et al, 2005). Only the wild-type amplicon was detected (1050bp), whereas the amplicon obtained by aberrant splicing (724bp) was not.

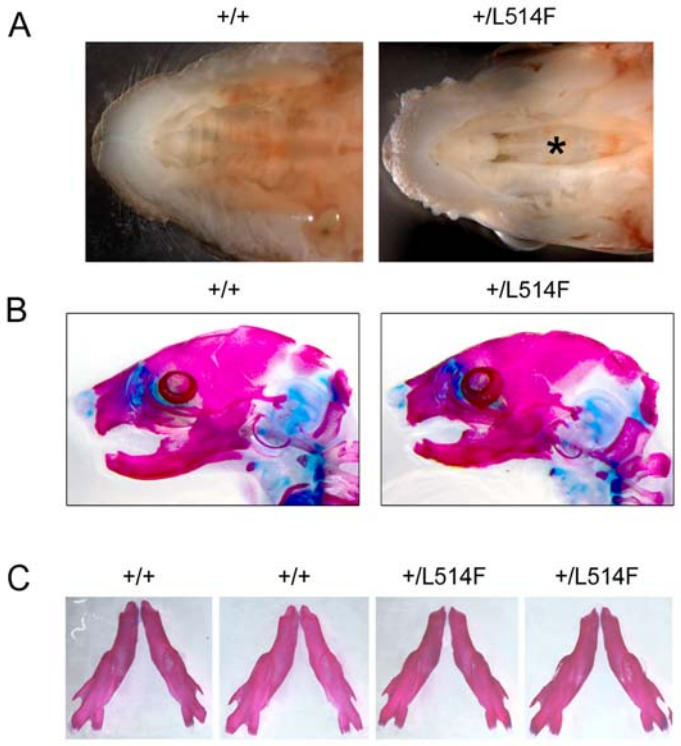

Figure S2. *p63*$^{+/L514F}$ mice are characterized by cleft palate with no other craniofacial abnormalities. (**A**) View of the newborn palate after removing the mandibles. * nasal cavity. (**B**) Craniofacial skeletons of newborn *p63*$^{+/L514F}$ and wild-type (+/+) mice stained for bone (alizarin red) and cartilage (alcian blue). (**C**) Isolated mandibles stained as in (B).

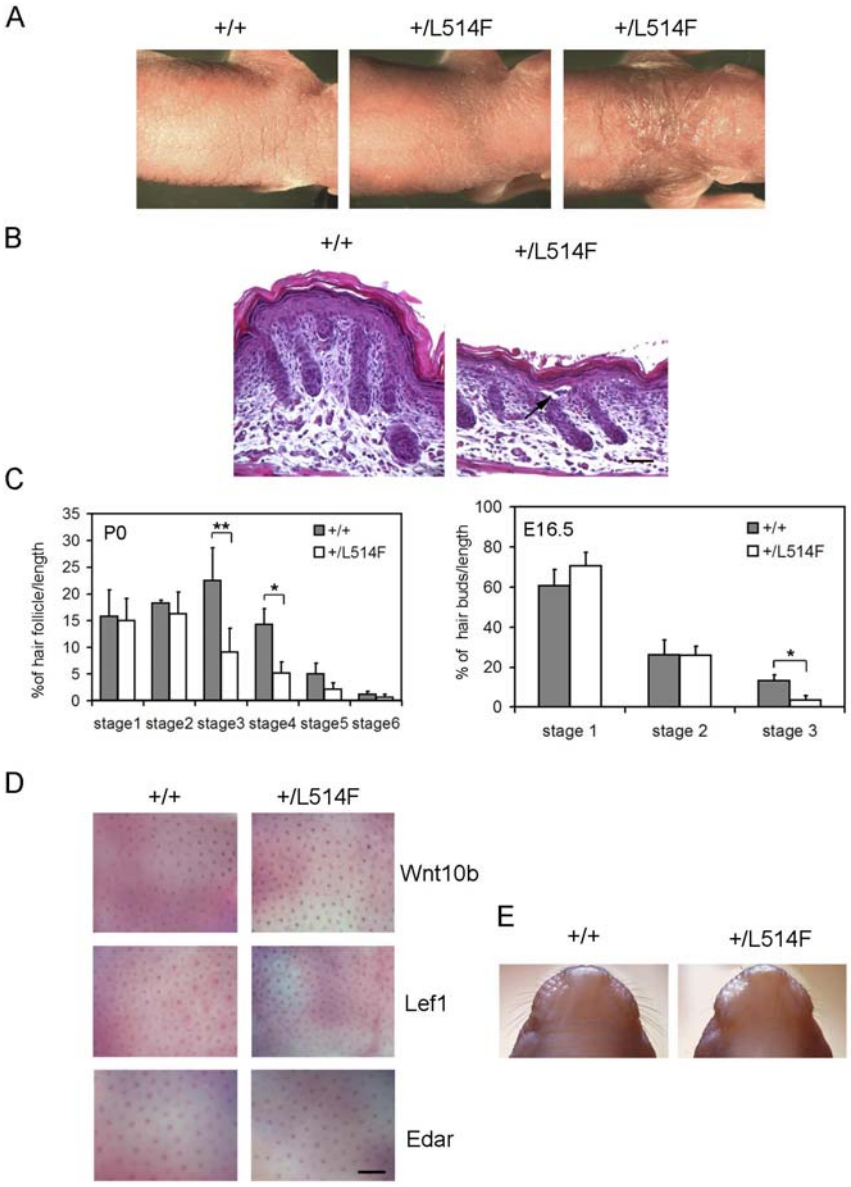

Figure S3. *p63*$^{+/L514F}$ mice are characterized by skin defects and ectodermal dysplasia. (**A**) Macroscopic appearance of *p63*$^{+/L514F}$ and +/+ dorsal skin. A severe phenotype is observed occasionally (right panel). (**B**) H&E staining of dorsal skin of *p63*$^{+/L514F}$ mice at P0. Blistering skin lesions localized mainly between the basal and the suprabasal layers (arrows) are observed in 21% of *p63*$^{+/L514F}$ newborn mice (n=28). (**C**) The number of well-developed hair follicles is reduced in *p63*$^{+/L514F}$ newborn mice and E16.5 embryos compared to controls. Stages of hair morphogenesis were measured as previously described (Paus et al, 1999). Left panel *p-value=0.0012; **p-value=0.0009; n=6. Right panel *p-value= 0.0106; n=6. Error bars denote SD. (**D**) Edar, Wnt10b and Lef1 expression detected by whole mount *in situ* hybridization is unaffected in mutant embryos at E14.5. Scale bar: 200 μm. (**E**) *p63*$^{+/L514F}$ mice have reduced vibrissae compared to controls.

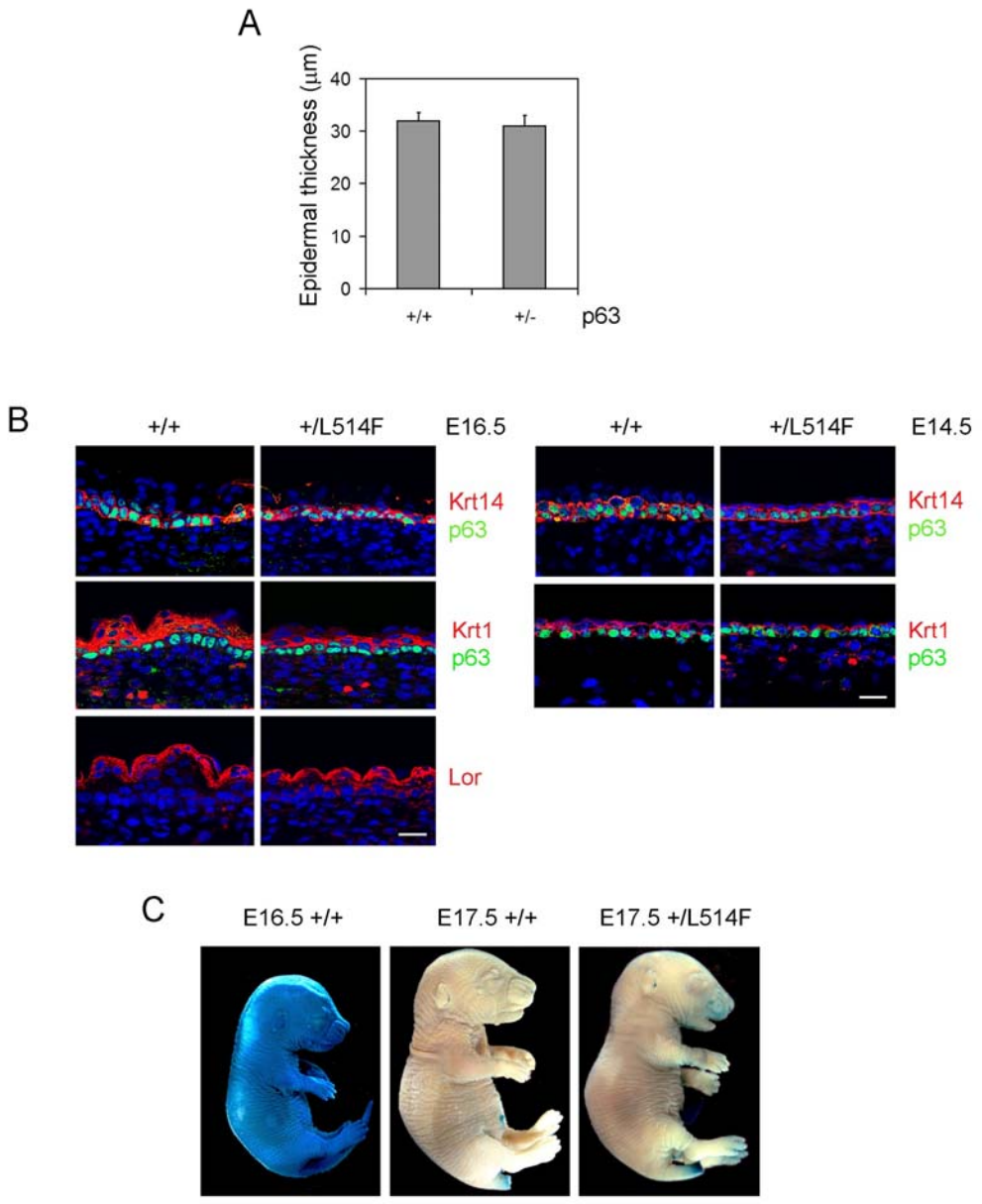

Figure S4. Unaffected epidermal stratification and skin barrier formation in *p63*$^{+/L514F}$ mutant embryos. (**A**) Quantification of epidermal thickness (μm) in p63$^{+/+}$ and p63$^{+/-}$ skin at birth (*p-value=0.559; n=6). Data are represented as mean +/- SD. (**B**) Immunostaining for the indicated differentiation markers in *p63*$^{+/L514F}$ embryos at E16.5 compared to controls. Scale bar: 20 μm. (**C**) Immunostaining at E14.5. Scale bar: 20 μm. (**D**) Skin barrier formation assay. At E17.5 *p63*$^{+/L514F}$ mice have a complete skin barrier formation as indicated by the lack of X-gal uptake. Wild-type embryos (+/+) before and after completion of the epidermal barrier are shown as control.

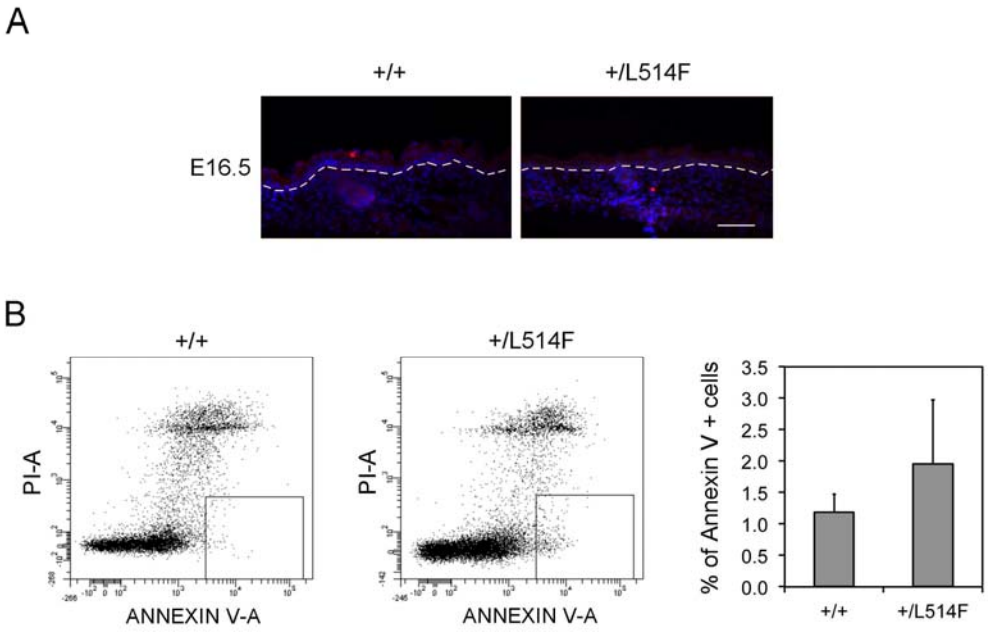

Figure S5. (**A**) Immunofluorescence for active caspase 3 at E16.5 showing low levels of apoptosis in *p63*$^{+/L514F}$ epidermis compared to wild-type. Arrows indicate apoptotic cells Scale bar: 50µm. (**B**) Left panel: representative FACS analysis of freshly isolated newborn epidermal cells immunostained with Annexin V antibody (x-axis) and Propidium iodide control reagent (y-axis). The box indicates apoptotic cells. Right panel: quantification of Annexin V positive cells (p-value= 0.11; n=12). Error bars denote SD.

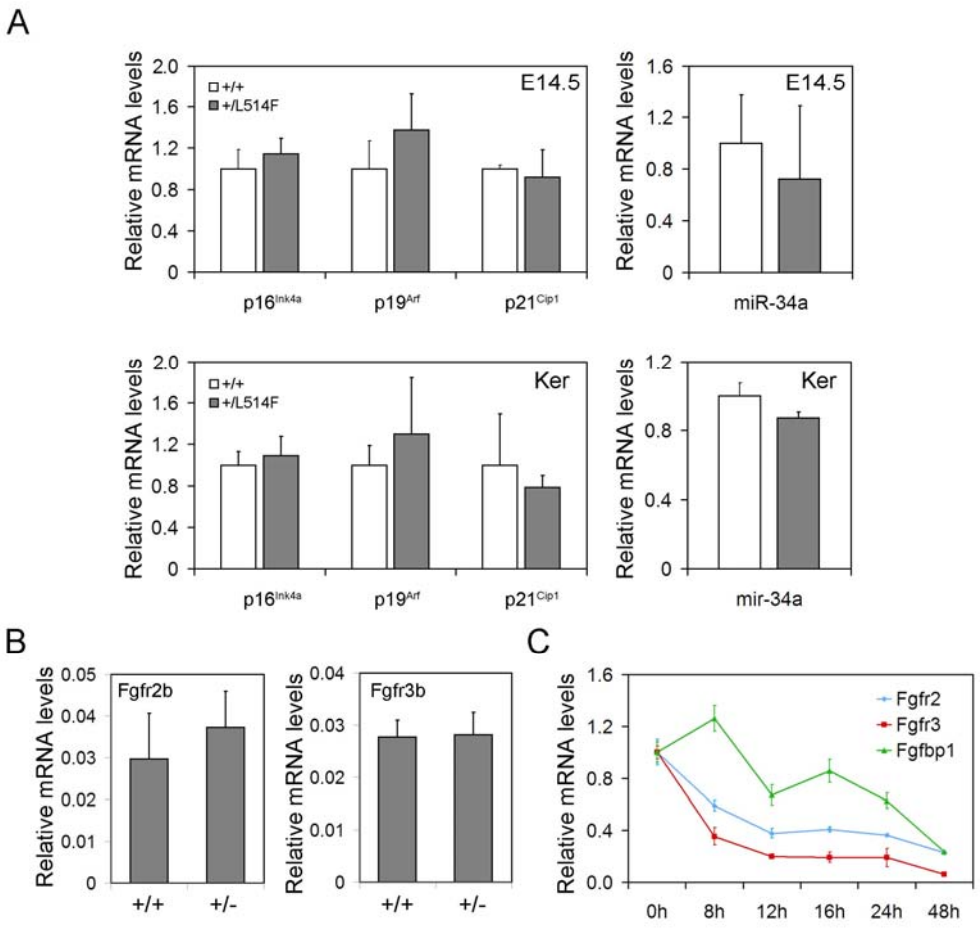

Figure S6. (**A**) Expression of the indicated cell cycle regulators in *p63*$^{+/L514F}$ E14.5 skin (upper panels) or primary keratinocytes (lower panels) is similar to controls. miR-34a expression was detected as previously described (Antonini et al, 2010). Error bars denote SD. (**B**) Real time RT-PCR performed on total RNA isolated from neonatal keratinocytes reveals similar expression of *Fgfr2b* and *Fgfr3b* in *p63*+/- compared to +/+ controls. Values are expressed as ß-actin normalized mRNA levels and are the mean of 4 independent epidermal samples. Error bars denote SD. (**C**) Real time RT-PCR for the indicated genes in keratinocytes at different times (h:hours) after transfection with p63-specific siRNA. Each time point was normalized for the corresponding control (0h) siRNA sample. Error bars denote SD.

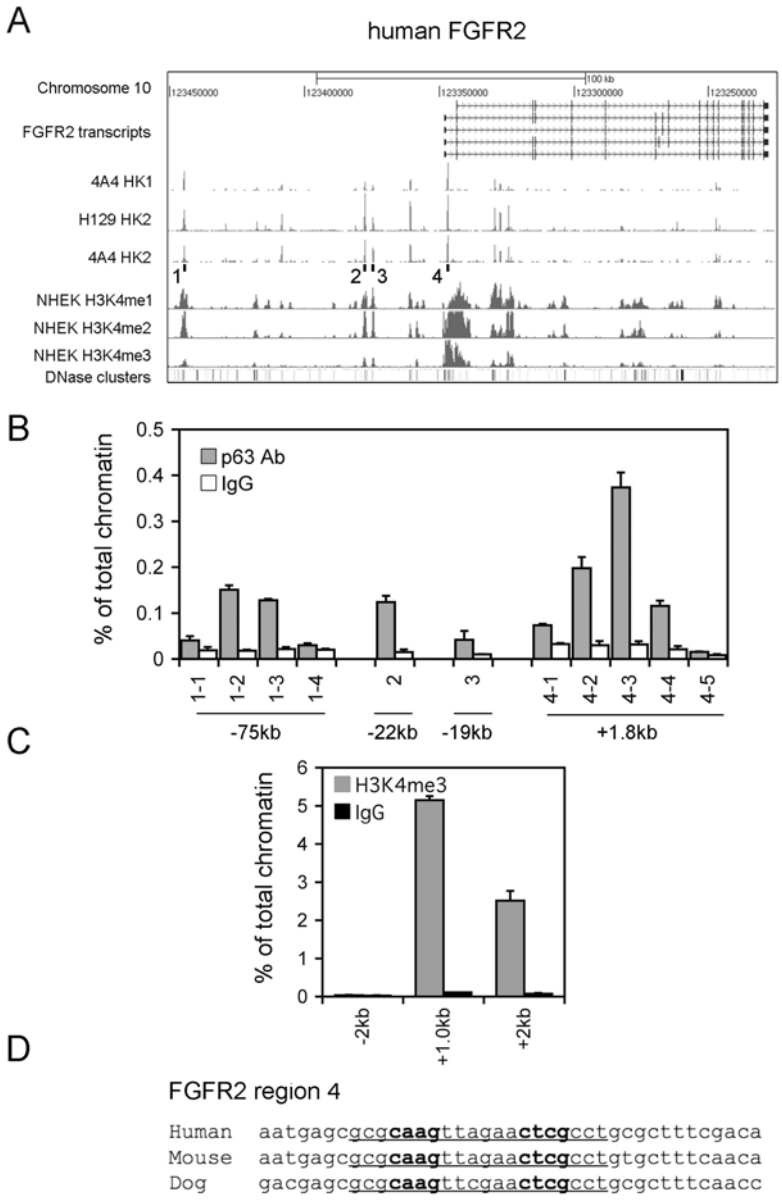

Figure S7. Identification of p63 binding regions in the *Fgfr2* gene locus. (**A**) The position of the p63 binding regions in the *FGFR2* genomic locus (numbered black bars) was obtained in human primary keratinocytes by ChIP-seq using 4A4 and H129 antibodies (Kouwenhoven et al, 2010). Genomic regions enriched for H3K4me and DNAse clusters are ENCODE consortium data (Birney et al, 2007). (**B**) ChIP assay performed on mouse primary keratinocytes using anti-p63 antibody (H137) and rabbit IgG on the *Fgfr2* genomic regions corresponding to the human p63 binding regions. Data are representative of three independent experiments. Error bars denote SEM. (**C**) ChIP assay performed on mouse primary keratinocytes using anti-H3K4me3 and rabbit IgG in a region spanning the +1.8kb p63 responsive region. A genomic region at -2kb from the TSS was used as negative control. Data are representative of three independent experiments. Error bars denote SEM. (**D**) Sequence of the most conserved p63 binding motif (underlined)

identified within region 4. The core consensus is in bold. See Table S4 for oligonucleotide primer sequences.

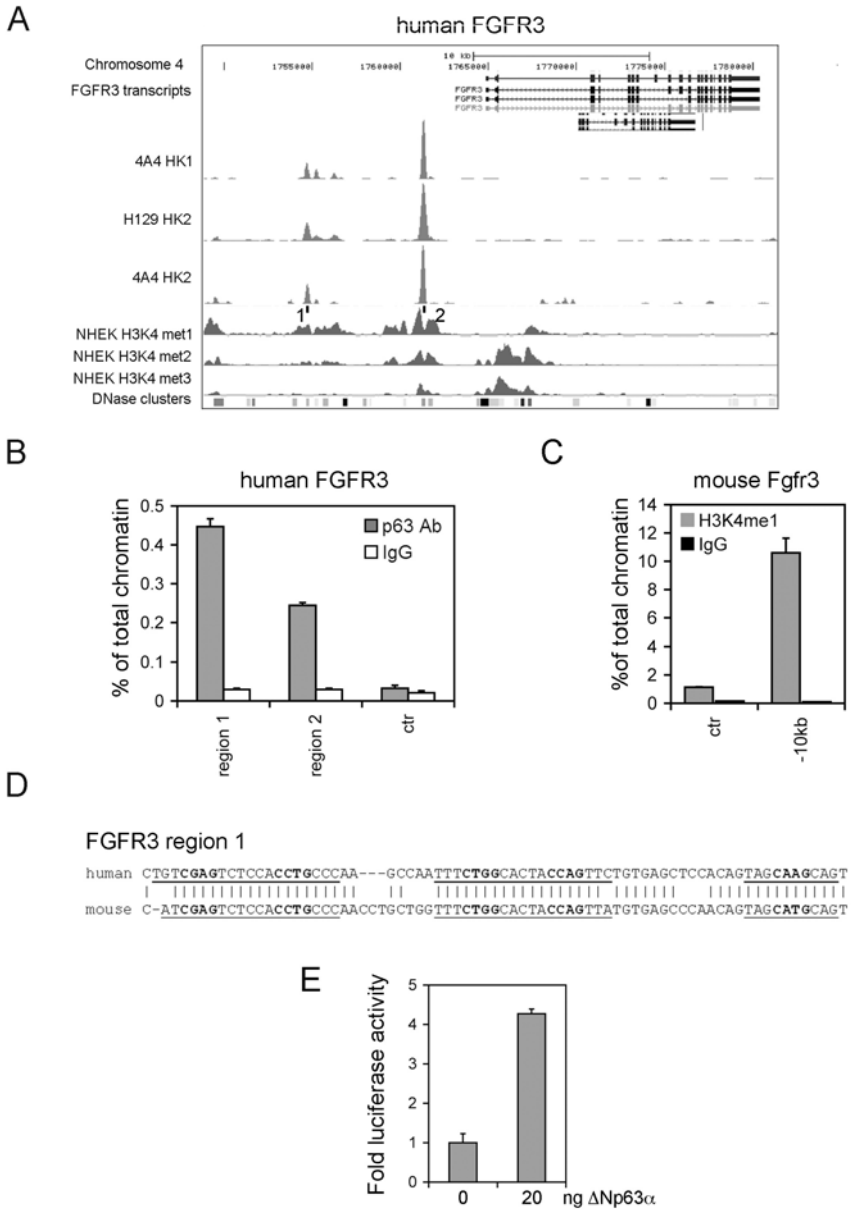

Figure S8. Identification of p63 binding regions in the *Fgfr3* gene locus. (**A**) The position of the p63 binding regions in the *FGFR3* genomic locus (numbered black bars) was obtained as in Figure S5A. (**B**) ChIP assay performed on human primary keratinocytes using anti-p63 antibody (H137) and rabbit IgG. A genomic region at -1.5kb from the TSS was used as negative control (ctr). Data are representative of three independent experiments. Error bars denote SEM. (**C**) ChIP assay performed on mouse primary keratinocytes using anti-H3K4me1. (**D**) The sequence of the

most conserved p63 binding motif (underlined) identified within region 1. The core consensus is in bold. See Table S4 for oligonucleotide primer sequences. (**E**) Luciferase assay reveals induction of *Fgfr3* enhancer activity (a 258bp genomic fragment encompassing the p63 binding region) in the presence of ΔNp63α in H1299 cells. Data are representative of three independent experiments. Error bars denote SEM.

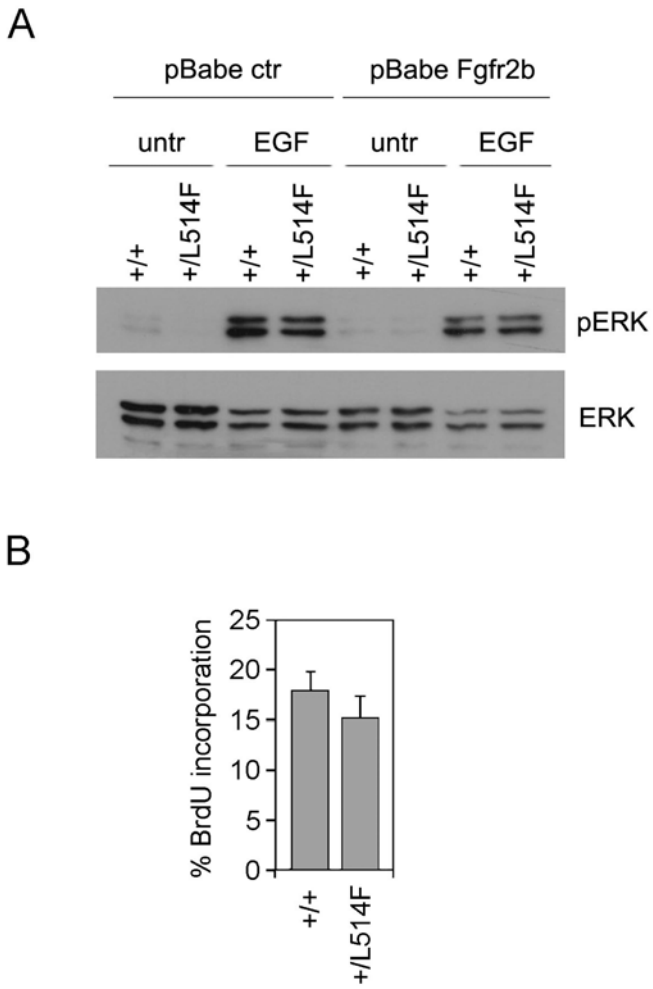

Figure S9. (**A**) Immunoblotting analysis for ERK phosphorylation reveals similar ERK activation in starved *p63*$^{+/L514F}$ keratinocytes compared to wild-type controls upon EGF treatment. Total ERK protein levels were used as control. (**B**) BrdU incorporation of primary keratinocytes grown for one-week in fully supplemented CnT-07 medium reveals a similar rate of cell proliferation between *p63*$^{+/L514F}$ and wild-type cells. Data are the means of three independent experiments. Error bars denote SEM.

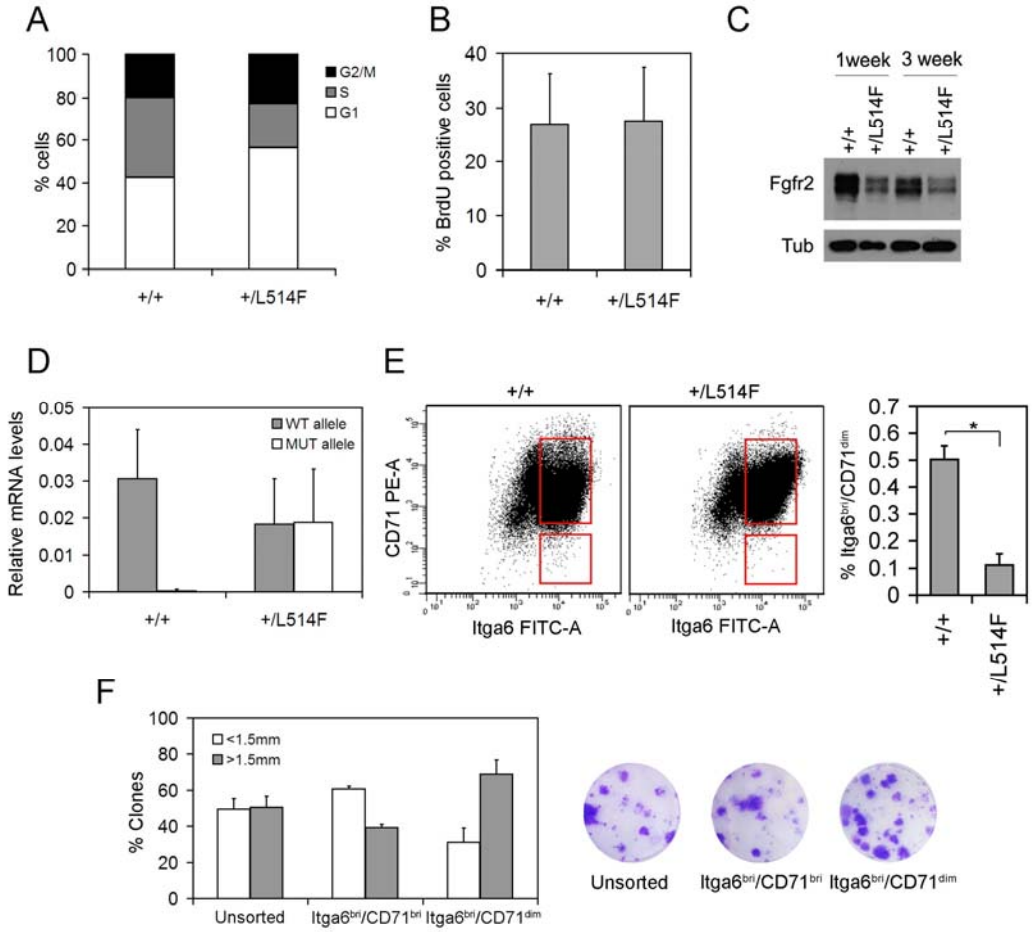

Figure S10. (**A**) FACS analysis of propidium iodide staining of *p63*$^{+/L514F}$mutant and +/+ cells grown one week under clonogenic conditions reveals a reduced number of cell in the S-phase of the cell cycle. Data are representative of two independent experiments. (**B**) BrdU incorporation of primary keratinocytes grown for three weeks under clonogenic conditions reveals a similar rate of cell proliferation between *p63*$^{+/L514F}$ and wild-type large colonies (<2mm; n=20). Error bars denote SD of two independent experiments. (**C**) Immunoblotting analysis reveals that reduced Fgfr2 protein levels in mutant keratinocytes are maintained at one and three weeks under clonogenic conditions. (**D**) Expression of mutant and wild-type p63 alleles by real time RT-PCR in *p63*$^{+/L514F}$ and +/+ cells at the third passage under clonogenic conditions reveals that mutant p63 is not lost in long term cultures (n=8). (**E**) FACS analysis of newborn epidermal cells immunostained with FITC-α6 integrin (x-axis) and PE-CD71 (y-axis) antibodies reveals a reduced number of putative stem cells (Itga6^{bri}/CD71^{dim}; bottom red rectangle) in *p63*$^{+/L514F}$ epidermis. Top red rectangle: transit-amplifying cells. Right panel: percentage of Itga6^{bri}/CD71^{dim} in *p63*$^{+/L514F}$ and +/+ epidermis (*p-value=10^{-6}; n=5). Error bars denote SD. (**F**) Itga6^{bri}/CD71^{dim} sorted keratinocytes have a higher clonogenic capacity than unsorted controls or Itga6^{bri}/CD71^{bri}. Data are representative of two independent experiments. Error bars denote SEM.

Table S1. Microarray analysis of p63 target genes at the indicated times during development and in keratinocytes.

probe set	Symbol	E14.5 MUT/WT	E18.5 MUT/WT	KER MUT/WT	p63KD/CTR	FDR E14.5	FDR E18.5	FDR KER	FDR p63KD
1418910_at	Bmp7	0.94	0.90	0.44	0.42	1.05	0.87	0.00	0.00
1424890_at	Bnc1	0.42	0.41	1.20	0.71	0.02	0.00	0.01	0.01
1437932_a_at	Cldn1	0.52	1.09	0.79	0.84	0.22	0.89	0.00	0.22
1450014_at	Cldn1	0.53	0.99	0.55	1.20	0.55	0.99	0.00	0.29
1419613_at	Col7a1	0.96	0.48	0.80	0.52	1.05	0.00	0.12	0.00
1422037_at	Dlx3	0.61	1.14	0.79	1.04	1.05	0.88	0.12	0.88
1449863_a_at	Dlx5	0.45	1.10	0.60	1.19	0.15	0.92	0.03	0.51
1421117_at	Dst	0.39	0.59	0.58	0.32	0.03	0.02	0.00	0.00
1450119_at	Dst	0.33	0.62	0.60	0.33	0.00	0.03	0.00	0.00
1433489_s_at	Fgfr2	0.64	0.73	0.52	0.52	0.18	0.22	0.00	0.00
1420847_a_at	Fgfr2	0.69	1.01	0.45	0.74	0.59	0.99	0.00	0.01
1425796_a_at	Fgfr3	0.74	0.74	0.64	0.34	0.96	0.75	0.29	0.00
1421841_at	Fgfr3	0.57	0.76	0.32	0.42	0.11	0.36	0.00	0.00
1423062_at	Igfbp3	1.19	0.97	5.79	1.79	0.84	0.99	0.00	0.00
1418301_at	Irf6	0.55	0.91	0.67	0.52	0.02	0.84	0.00	0.00
1426431_at	Jag2	0.67	0.75	0.69	0.49	0.49	0.50	0.00	0.00
1455573_at	Krt14	0.62	0.86	1.16	0.53	0.34	0.77	0.08	0.00
1460347_at	Krt14	0.45	0.74	1.03	0.91	0.00	0.13	0.32	0.00
1423935_x_at	Krt14	0.53	0.88	1.02	0.93	0.00	0.53	0.54	0.01
1418634_at	Notch1	0.74	0.64	0.97	0.38	0.35	0.03	0.65	0.00
1418633_at	Notch1	0.61	0.64	0.90	0.54	0.11	0.11	0.24	0.00
1416271_at	Perp	0.73	1.05	0.93	0.82	0.08	0.72	0.01	0.00
1454773_at	Rxra	0.71	1.04	0.64	0.82	0.50	0.96	0.00	0.21
1448612_at	Sfn	0.50	0.81	0.57	0.67	0.04	0.41	0.00	0.00
1423389_at	Smad7	1.00	1.21	1.81	2.36	1.03	0.80	0.00	0.00
1426048_s_at	Tcfap2a	0.70	1.20	0.88	1.03	0.53	0.61	0.05	0.85
1450782_at	Wnt4	0.87	0.81	0.34	0.54	1.02	0.61	0.00	0.00

MUT/WT: ratio between gene expression in $p63^{+/L514F}$ versus +/+ cells or tissues. FDR: False Discovery Rate;

downregulated genes are in green; upregulated genes are in orange.

Table S2. Microarray analysis of genes encoding for FGF signaling components in embryonic epidermis at E14.5.

probe set	Gene Symbol	MUT/WT E14.5	FDR	WT1 E14.5	WT2 E14.5	MUT1 E14.5	MUT2 E14.5
1450869_at	Fgf1	0.86	1.05	62	87	73	56
1423136_at	Fgf1	1.01	1.03	81	49	62	69
1420690_at	Fgf10	0.73	0.92	103	82	42	93
1439959_at	Fgf11	1.02	1.04	166	227	202	198
1451693_a_at	Fgf12	1.10	1.05	18	33	30	26
1418498_at	Fgf13	1.16	1.06	61	39	51	66
1418497_at	Fgf13	1.32	0.71	476	443	543	667
1420806_at	Fgf16	0.85	1.05	28	7	17	13
1421523_at	Fgf17	0.78	0.88	129	131	102	101
1449545_at	Fgf18	1.00	1.03	42	98	73	66
1449826_a_at	Fgf2	0.30	0.46	15	12	7	1
1421677_at	Fgf20	0.72	0.87	56	36	32	34
1422916_at	Fgf21	0.88	1.06	28	19	25	16
1422176_at	Fgf23	0.78	1.05	4	9	8	2
1441350_at	Fgf3	0.67	0.91	33	24	20	18
1422923_at	Fgf3	0.89	1.05	17	29	18	23
1449729_at	Fgf4	0.74	1.05	1	6	4	1
1450282_at	Fgf4	1.08	1.05	203	176	215	193
1427582_at	Fgf6	0.97	1.04	59	70	55	71
1422243_at	Fgf7	1.11	1.06	175	96	149	152
1420795_at	Fgf9	1.23	0.88	73	75	90	93
1419086_at	Fgfbp1	0.59	0.17	2971	2195	1954	1116
1424050_s_at	Fgfr1	0.99	1.03	886	992	783	1083
1425911_a_at	Fgfr1	1.07	1.05	80	116	95	115
1427526_at	Fgfr1op2	0.84	0.99	300	392	336	243
1423591_at	Fgfr1op2	0.95	1.05	2051	1856	1838	1862
1431020_a_at	Fgfr1op2	1.22	1.02	681	289	637	545
1433489_s_at	Fgfr2	0.64	0.18	1235	1597	889	914
1420847_a_at	Fgfr2	0.69	0.59	310	251	206	182

1421841_at	Fgfr3	0.57	0.11	489	514	333	241
1427777_x_at	Fgfr4	0.87	1.06	80	83	62	80
1427846_x_at	Fgfr4	1.10	1.06	91	99	115	93
1418596_at	Fgfr4	1.41	0.55	120	136	161	199
1427776_a_at	Fgfr4	1.50	0.90	25	42	33	68
1451912_a_at	Fgfrl1	1.39	0.58	248	299	322	435

FDR: False Discovery Rate; significant downregulation is indicated in green

Table S3. Mutations in AEC patients used in this study.

Patients	DNA mutation	Protein mutation	Exon	Sample
AEC 1	c.1630G>T	D544Y	14	RNA
AEC 2	c.1682G>T	G561V	14	RNA
AEC 3	c.1578C>A	F526L	13	RNA
AEC 4	c.1631A>T	D544V	14	RNA
AEC 5	c.1578C>A	F526L	13	RNA
AEC 6	c.1610T>C	I537T	13	RNA
AEC 1	c.1630G>T	D544Y	14	paraffin
AEC 2	c.1555T>C	C519R	13	paraffin

Table S4. List of oligonucleotide primers used in this study.

Oligonucleotide primers for miniarms generation by Recombeneering method

SET	Forward primer (5'-3')	Reverse primer (5'-3')
-*Not*I-p63ex12For -*Hin*dIII-p63ex12Rev	ATAAGCGGCCGCCAGGATGCTGC TGGTGATAA	GTCAAGCTTGGAGCCACAA TAGCCCTGTA
-*Hin*dIII-p63-3'UTRFor -*Spe*I-p63-3'UTRRev	GTCAAGCTTTGCAAAAGCAAATGA GTCCT	TCTACTAGTGGAATCCCATT CTCCACTGA
-NotI-ex13For -EcoI-ex13Rev	ATAAGCGGCCGCCAAATCGCCAG CTGAAAAAT	GTCGAATTCCGAGGTTCTG ACCTGGAGAG
-*Bam*HI-intron13For -*Sal*I-intron13Rev	ATAGGATCCGCAATCAATATGCCT GATCCT	GTCGTCGACTTTCTGCTCTC CTGCCTGAT

Oligonucleotide primers for ES cell screening and mouse genotyping

Screening	Forward primer (5'-3')	Reverse primer (5'-3')
Es 5'	CAGACTGCAGCATTGTCAGGTGAG	GCTAGCTTGGCTGGACGTAAACTC
Es 3'	ATGGCTTCTGAGGCGGAAAGAACCAG	AGGCCAGAGGTCAGAAGGATGAACAC AC
p63 wt	GTCTGACCTCCCGACCCACCTCCT	GCATGATGAGCAGCCCAACCTTGCT
p63 mut	GTCTGACCTCCCGACCCACCTCCT	GCATGATGAGCAGCCCAACCTTGCA

Oligonucleotide primers for Real Time RT-PCR on mouse samples

Gene	Forward primer (5'-3')	Reverse primer (5'-3')
ß-actin	CTAAGGCCAACCGTGAAAAGAT	GCCTGGATGGCTACGTACATG
p63 ex13 wt	GAGCAGCCCAACCTTGCT	ACTCTCCATGCCCTCCAC
p63 ex13 mut	GAGCAGCCCAACCTTGCA	ACTCTCCATGCCCTCCAC
Fgfr2	TGGGCTGCCCTACCTCAAG	GCACTTCTGCATTGGAGCTATTT
Fgfr3	CCTTTTGGCTGCGTGTTCA	CAGCCTCATCAGTTTCCATCAG
Fgfbp1	TCCCCAGTACACCTGGATCTG	TGAGGCTGTGGAGTCTCATCAC
$p16^{Ink4a}$	CCCAACGCCCCGAACT	CGTGAACGTTGCCCATCA
$p19^{Arf}$	TGGACCAGGTGATGATGATG	CGAATCTGCACCGTAGTTGA
$p21^{Cip1}$	GAACATCTCAGGGCCGAAAA	CAATCTGCGCTTGGAGTGAT
Fgfr2-intron 6 (pre-mRNA)	CCAATGTGGAGGTTGGAAACA	CAGCTAAGAGCACGCATTGC
Fgfr2-intron 1 (pre-	AATGAGCGCGCAAGTTAGAAC	GCCGCGCCGAGATGT

mRNA)		

Oligonucleotide primers for Real Time RT-PCR on human samples

Gene	Forward primer (5'-3')	Reverse primer (5'-3')
RPLP0	GACGGATTACACCTTCCCACTT	GGCAGATGGATCAGCCAAGA
Krt15	ACCACGAAGAGGAGATGAAGGA	TGCGTCCATCTCCACATTGA
Sox9	CAAGAAGGACCACCCGGATT	GCCCGTTCTTCACCGACTT

Oligonucleotide primers for RT-PCR on mouse samples

Gene	Forward primer (5'-3')	Reverse primer (5'-3')
p63	GAAACCAGAGATGGGCAAGTCCT	CTCTTTGATACGCTGCTGCTTG

Oligonucleotide Primers for ChIP analysis on mouse

SET	Kb from TSS of Fgfr2	Forward primer (5'-3')	Reverse primer (5'-3')
1-1	77 up	GCCACATGGACGAGAACACA	TGGGAGGCAAGGGTTCAG
1-2	76.3 up	TCAGCCCCTTCCTTGAGTGT	GGGACAGAAATCTTCTCTGGAATTT
1-3	76.2 up	CGCCAGCAGCTCAGAACAG	GGCTACCCGTGTCATTTTAAACTAG
1-4	75.8 up	TAGGGTCTTGCCTACTTTCTATTAATTTTC	AAGGCATGCACAACTTCTTGAG
1-5	75 up	CCTCATCAAGGACACTTCTCTTTG	GGCTCTGCATATTGCTTGTCTGT
3	22 up	CACACATGCCTTTACTTGCTAAGAG	CGATCACACTTTGTTTGGGACAT
4	19 up	TGGGCATCTCTGGGAATCTG	GGGCATGTTTCAGCTTGATAATTAT
6-1	1.8 down	GCCATCCGCATTCATCCA	CGCACCCTGTCAGTCTCTGA
6-2	1.8 down	GCCACTGCCTCCCTAAAGGT	CAGGCAACATCCCCAAAGG
6-3	1.8 down	AATGAGCGCGCAAGTTAGAAC	GCCGCGCCGAGATGT
6-4	1.8 down	GGGCGCCTGATTGCTTT	CAGCCTGGACTCATTTTCATCTG
6-5	130 up	ACTCTGACGGATGGCTCTTCA	AGGCAGACTTGTGTGGAGATGA

SET	Kb from TSS of Fgfr3	Forward primer (5'-3')	Reverse primer (5'-3')

-10kb	10 up	AGACGAGGCAGGTGGAGTTG	CTGCCCTGAACCTCCTGTTC
ctr	8.5 up	AGGCTCTTGTGGCTTCCAGAT	CACCTGGCCCTGTCCTGTA

Oligonucleotide Primers for ChIP analysis on human

SET	Kb from TSS of Fgfr3	Forward primer (5'-3')	Reverse primer (5'-3')
Region2	10 up	ACAGGCTGGCTGTCGAGTCT	CACAGAACTGGTAGTGCCAGAAA
Region3	3 up	TAAACCGGAGTCCAGCAGATG	CATGTGCAGGAGGCTCCAA
ctr	1.5 up	CGCATGCTGGTGCTTTCA	GGATTGCAGGTGTGAGCTCTCT

Oligonucleotide primers for Histone H3 ChIP analysis on mouse

H3K4	Kb from TSS	Forward primer (5'-3')	Reverse primer (5'-3')
me1	-50kb (Fgfr3)	AGCTGGTGGCCAAAACAGAT	GGAAGGCAGGACAGGGTATG
me1	-10kb (Fgfr3)	GGATCCTTAGGTCTGTGTTGCAA	CCCCCACATCTGCTCTCAA
me2-3	-2kb (Fgfr2)	TCCATCCTGAGGAGCAAACG	GGCCCCTTTCCTCCTCTTCT
me2-3	+1kb (Fgfr2)	GCCATCCGCATTCATCCA	CGCACCCTGTCAGTCTCTGA
me2-3	+2kb (Fgfr2)	GGGCGCCTGATTGCTTT	CAGCCTGGACTCATTTTCATCTG

Oligonucleotide primers for mutagenesis of the p63 binding site in *Fgfr2* regulatory region

Kb from TSS	Forward primer (5'-3')	Reverse primer (5'-3')
+1.8kb)	TGAAAGAATGAGCGCG**GG**AGTTAGA ACTCGCCTGTG*	CACAGGCGAGTTCTAACTCCCGCGCTC ATTCTTTCA

* underlined in bold is the 2bp mutation. The p63 binding core CAAG was mutated in GGAG.